Building a Whole Spine from Segments: Lumbar Spine Response during Dynamic Compression

Maria A. Ortiz-Paparoni, Michaela Pigue, Cameron R. 'Dale' Bass

Abstract Development of injury mitigation techniques for dynamic compression of the spine relies on local dynamic response. Attention needs to be paid to the ability of the material model to capture rate-dependent responses of the spine, and to the attainment of whole spine models based on FSU data. This study assesses the influence of dynamic compression rates on the behaviour of the thoracolumbar spine and spinal segments as well as the relationship of spinal segments to the thoracolumbar spine response. Post-mortem human subject thoracolumbar spines and FSUs from the same donors were subjected to three dynamic compression rates of 200, 400, and 600 N/ms resulting in an average thoracolumbar stiffness of 360 ± 93, 424 ± 99, 505 ± 106 N/mm. No statistically significant differences on stiffness across the proposed loading rates was observed for thoracolumbar spines or FSUs. A nonlinear FSU response (fourth order polynomial) improved the full spine reconstruction by 28.6% over a linear model. Though the nonlinear model underpredicted the thoracolumbar response, the deviation from the mean of the composite spine overlapped with the standard deviation of the thoracolumbar experimental response. The normalised deviation from the mean between the nonlinear reconstruction and the thoracolumbar spine averaged 8.4%.

Keywords Dynamic compression, lumbar spine, rate dependency, whole spine modeling.

I. INTRODUCTION

Spinal trauma is a major issue with considerable societal, economic and physical consequences [1,2]. In recent years, dynamic compressive loading as an injury mechanism of the spine has gained attention due to the increased use of Improvised Explosive Devices (IEDs) in recent US military conflicts [3,4]. During Operation Iraqi Freedom and Operation Enduring Freedom spine injuries accounted for 5.5% of all casualties, the highest incidence of spine injuries than any other American military conflict [5]. The lumbar spine is a main region of interest during these dynamic injury scenarios, owing to the effect of spinal injuries on functional capacity and the load transmission mechanism of the compressive event. Previous studies have investigated the response of thoracolumbar spines [6-9] and lumbar functional spinal units (FSUs) [10-12] under dynamic compression conditions relevant to underbody blast. While the referenced studies provide valuable information from injury risks of the lumbar spine [9] to FSU strain rate behaviour [12], they have been limited in the investigation of compressive dynamic loading conditions of 200 N/ms, 400 N/ms, and 600 N/ms for both whole thoracolumbar spines (T12-S1) and FSUs obtained from the same donor. The proposed loading rates in this study can result in strain rates ranging from 1 – 9 s^{-1} for whole lumbar spines and spinal segments, corresponding to the lower end of under body blast loading regime reported by reference [13].

Furthermore, to develop an accurate dynamic characterisation of the spine, it is important to recognise its viscoelastic nature. While previous studies have studied the behaviour of the spine under low velocity loading conditions [14-17], its viscoelastic response to the proposed dynamic compressive loading has received less attention. The demonstration of relaxation time constants faster than 10 ms in cervical spine ligaments under high-rate loading [18] highlights the importance of determining the high-rate viscoelastic response of the spine.

Additionally, the development of injury mitigation techniques for dynamic compression of the spine can greatly benefit from understanding the local dynamic response. To that effect, anthropometric test device (ATD) designers and computational modellers need to be cautious when recreating whole spine models from segmental spine data. Reference [19] found that a linear prediction of the whole cervical spine stiffness (OC-C7) in tension using a linear combination of spine segment properties under the same conditions and from the same donor

M. A. Ortiz-Paparoni is a PhD candidate (tel: +1 919-660-5450, maria.ortiz@duke.edu), M. Pigue is a MSc graduate and C. R. 'Dale' Bass is an Associate Research Professor in Biomedical Engineering at Duke University in Durham, NC, USA.

resulted in 32% error, with the whole cervical spine stiffness always being greater than the stiffness reconstructed from spinal segments. References [20,21] found similar results, where the data suggest that combining the component level stiffness response under tensile loading of a cervical spine would not yield the response of the whole cervical spine under the same loading condition for the same donor. Currently it is unknown if a similar behaviour occurs in the thoracolumbar spine under dynamic compression.

By assessing the influence of a range of dynamic compression rates on the behaviour of the lumbar spine and spinal segments, as well as the relationship of spinal segments to the thoracolumbar spine response. This study provides data and an analytical model for FSU combination to improve multibody and finite element computational models, as well as ATDs, which can likely contribute to the development of injury mitigation and prevention techniques.

II. METHODS

The methodology for this paper can be separated into two sections: the dynamic compression testing of thoracolumbar (T12-S1) spines and FSUs, and the analytical models derived to investigate the combination of lumbar FSU responses to recreate a thoracolumbar spine response.

Whole Spine and FSU Testing

This study was performed in compliance with the Duke University Institutional Review Board approved post-mortem human subject (PMHS) research protocol, Durham, NC, USA. Three PMHS lumbar spines were dissected from whole body male donors. Demographic data available for all the specimens included age (74 ± 6.9 years), and weight (74.8 ± 25.6 kg). Heights of two out of the three specimens were available, corresponding to 177.8 and 167.6 cm. To assess structural integrity of the thoracolumbar spine µCT images were generated at 100 µm x 100 µm x 100 µm resolution (Nikon Metrology Inc., Model XTH 225 ST, Brighton, MI, 48116). Specimens were kept frozen at -20 °C to avoid degradation, and were thawed at room temperature the day prior to preparation. This preservation procedure has been reported to have no significant effect on the mechanical properties of the annulus fibrosus of the intervertebral discs (IVDs), bone, or ligaments [22-24].

Thoracolumbar spines were dissected to the T11-S1 vertebra. Ribs, musculature, fat, and periosteum were excised carefully to allow fixation, sensor placement, and vertebral body visualisation. To create a rigid fixation amongst bony components and casting materials, screws and k-wires were inserted into the T11 vertebral body and S1 without influencing IVDs and other joint components of T12-L1 and L5-S1. Following wire and screw insertions, T11-T12 and S1 were wrapped with polymethylmethacrylate (PMMA) to provide rigid attachment points, distribute stress, and provide further surface adherence to casting materials. The ends of the whole spine specimens (T11-T12 and S1) were then cast in aluminum mounting cups using a fast curing resin (Golden West Mfg., Inc., Grass Valley, CA 95945). The thoracolumbar spine was aligned to match the description of the nominal posture provided by the seated soldier study [25], with the mid vertebral body of T12 at 2° in extension, the S1 superior endplate at 10° extension, and the spinal angle (inferior endplate of T12 to superior endplate of S1) at 11.5° rearward from the vertical. The specimen was then placed in a servohydraulic Materials Testing Machine (MTS®, 22 m/s maximum velocity, Eden Prairie, MN) with the cranial end (T11-T12) fixed at the MTS crosshead, and the caudal end (S1) attached to the hydraulic actuator (Figure 1). Once the specimen was positioned in the MTS, superior and inferior endplate angles at all spinal levels were measured with an inclinometer and recorded to replicate segment posture in FSU testing. Similarly the spinal inclination angle in the sagittal plane was recorded for all the FSUs to be replicated during segment testing. To avoid dehydration the specimens were maintained in saline soaked gauze during tissue preparation and were continuously hydrated with physiological saline during testing.

To provide physiological conditioning for the spines, specimens were preconditioned for five minutes with a 1 Hz oscillatory pulse at 1% strain, which resulted in an average peak compressive force of 985 ± 235 N that has been reported to be within the range of compressive forces experienced by the lumbar spine during walking [26]. Following preconditioning, thoracolumbar spines were subjected to three non-injurious dynamic compression conditions at rates 200 (V1), 400 (V2), and 600 (V3) N/ms. Rest intervals between tests were set to 10 min to allow viscoelastic relaxation and compression rates were tested twice to ensure response repeatability. Once the high rate test (V3) was completed the lowest rate baseline test (V1) was repeated to ensure no injury occurred during compression. Following the thoracolumbar spine tests, the spine was divided into FSUs. While two of the lumbar spines were divided into T12-L1, L2-L3, and L4-L5 FSUs, one of the spines was divided into T12-L1, L2-L3, and L4-S1 FSUs due to a calcified fusion of the L5-S1 intervertebral joints. The segments were cast in the same manner as the thoracolumbar spine with screws, k-wire, and PMMA, in mounting cups with the fast curing resin. Segment postures were matched to recorded FSU positioning during thoracolumbar testing, with the spinal and superior endplate angles being prioritized over the inferior endplate angle. The functional spinal units were subjected to the same test matrix of preconditioning, and compressive rates of V1, V2, and V3 as the thoracolumbar spine in the MTS (Figure 2). The force and displacement responses for both whole spine and FSU tests were recorded by a 6-axis load cell (AMTI, Watertown, MA 02472, USA) at the superior condition, and a linear variable displacement transducer (LVDT) (Measurement Specialties, Hampton, VA 23666, USA) at the hydraulic actuator. Data was collected at 100 KHz, and filtered with a 3000 Hz, 8-pole low-pass Butterworth filter to consider higher frequency components than in SAE J211 CFC 1000 used for impact testing. The axial force and displacement data was corrected with a nonlinear compliance function to account for fixation compliance within the specimen casting [19]. The linear portion of the compliance curve presented a stiffness of 6338 ± 166 N/mm (n = 11).

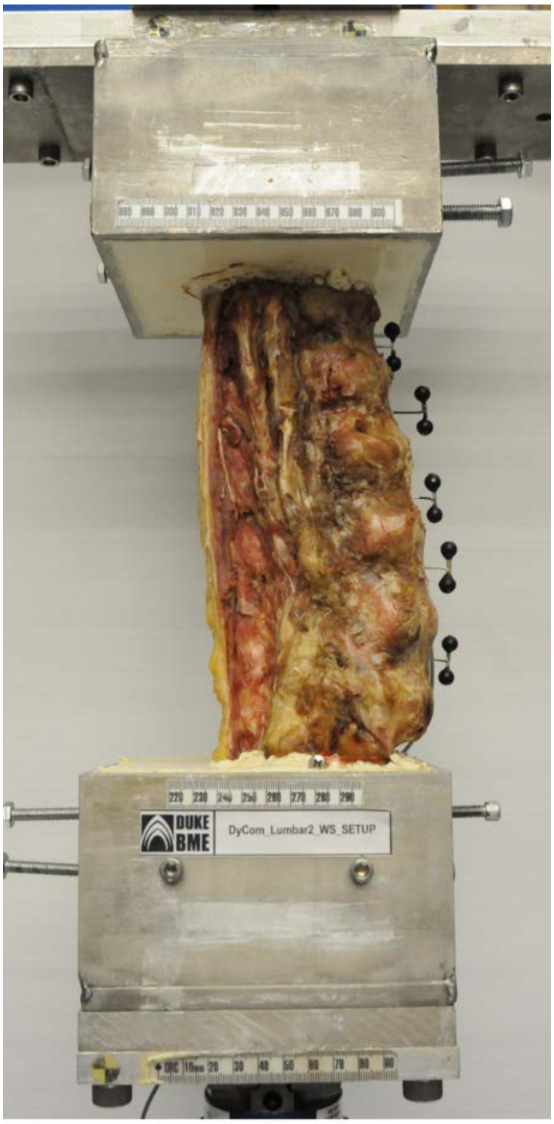

Fig. 1. Mounting of a whole spine specimen. Fixation ends (T11-T12, and S1) embedded in aluminum cups with fast curing resin. Cranial end (T11-T12) attached to superior fixed end condition of the MTS, caudal end (S1) attached to hydraulic actuator.

Fig. 2. Mounting of T12-L1 FSU to servohydraulic materials testing machine. Portions of the FSU's superior and inferior vertebral bodies are embedded in fast curing resin while allowing joint elements to be unconfined by fixation.

Analytical models

To investigate the effects of loading rate on both segments and thoracolumbar response, a stiffness metric was defined as the linear regression of 20% - 80% of the force vs. displacement curve. The region of interest of the force-deflection curve was selected to avoid effects induced by the small amplitude specimen nonlinearity (often called the toe-region) and the large amplitude changing viscoelastic response from the deceleration of the piston when reaching maximum displacement. Linear regression coefficients (R^2) were used to assess the goodness of the linear representation of the spine stiffness response and a one way Anova was used to determine the influence of loading rate on both thoracolumbar spine and segment stiffness. To assess FSU compressive stress (σ) behaviour the axial force at 80% of the force-displacement curve was divided by the FSU's IVD cross sectional area (CSA), for whole lumbar spine specimens the CSA was calculated as the average of the T12-S1 FSUs.

Accounting for differences in the nonlinear viscoelastic response of the segments tested individually, compared with segments tested as a part of the thoracolumbar spine, is critical to reconstruct whole spine response from FSU data. Since the loading rates did not span an order of magnitude in strain rates, we assumed a hyperelastic response, i.e., minimal relaxation differences between tests across the time history of the loading, to model the nonlinear whole spine and component behaviour. This allowed more accurate replication of the stress-strain response in the composite model compared with the thoracolumbar model. For this, the isolated segmental response was modelled as a fourth order polynomial (Equation 1).

$$d_{ts} = a_i * {F_{ts}}^4 + b_i * {F_{ts}}^3 + c_i * {F_{ts}}^2 + e_i * F_{ts} \tag{1}$$

where d_{ts} is the modelled displacement response of a tested segment, F_{ts} is the compressive force to which the tested specimen is subjected, and a_i, b_i, c_i, and e_i are the fourth order polynomial coefficients that best represent the experimental response of the tested specimen. A list for the tested specimen coefficients is provided in the Appendix. Due to the nature of FSU testing not all segment responses can be obtained. Therefore, missing segment response was estimated as the normalised average of the modelled displacement of the tested segments that were above and below it, i.e., L1-L2 response was estimated to be the normalised average of the T12-L1 and L2-L3 modelled response. For the thoracolumbar spine that had a fused L5-S1 joint, the missing L3-L4 segment response was normalised only by the tested L2-L3 modelled response. Scale factors (SF) for normalisation of the missing segment response were based on mid-IVD CSA and height (H), and are given by Equations 2 and 3. Cross sectional area and mid-IVD height were determined through µCT scans of the thoracolumbar spine prior to testing. Slices that bisected the IVD in the axial plane and bisected the FSU on the sagittal plane were selected for CSA and IVD height measurements, respectively. Missing segment response is given by Equation 4.

$$SF_{sup} = {(H_{sup}/mean(H_{sup}, H_{inf}))}\Big/{(CSA_{sup}/mean(CSA_{sup}, CSA_{inf}))} \tag{2}$$

$$SF_{inf} = {(H_{inf}/mean(H_{sup}, H_{inf}))}\Big/{(CSA_{inf}/mean(CSA_{sup}, CSA_{inf}))} \tag{3}$$

$$d_{ms} = mean(d_{sup} * SF_{sup}, d_{inf} * SF_{inf}) \tag{4}$$

where d_{ms} is the modelled displacement of the missing FSU, and "sup" and "inf" indices denote properties associated to the tested FSUs that are superior and inferior to the missing segment, respectively.

Assuming all the segments undergo the same compression force during thoracolumbar spine testing, the displacement response of the composite whole spine was modelled as the summation of each tested segment modelled displacement and the normalised displacement response of missing segments. The scale factor for modelled displacement of missing segments is given by Equation 5 and reconstructed spine displacement response is given by Equation 6.

$$SF_{ms} = {(CSA_{ms}/mean(CSA_{sup}, CSA_{inf}))}\Big/{((H_{ms}/mean(H_{sup}, H_{inf}))} \tag{5}$$

$$d_{RS} = \sum d_{ts} + \sum d_{ms} * SF_{ms} \tag{6}$$

where "ms" index denotes quantities associated to the missing FSU, d_{RS} is the displacement of the reconstructed spine, and d_{ts} is the modelled displacement of the tested segments.

The normalised deviation from the mean ($Mean_{DEV}$) (Equation 7) between the modelled experimental thoracolumbar response and the reconstructed spine was used to assess the suitability of the proposed composite spine model.

$$Mean_{DEV} = \frac{mean(d_{EM}) - mean(d_{RS})}{mean(d_{EM})} \tag{7}$$

where d_{EM} is the displacement of the fourth order polynomial fit of the experimental whole spine data, d_{RS} is the displacement of the composite spine, and the mean is taken across the three lumbar spines tested.

III. RESULTS

Loading Rate Effects

The stiffness of the spine was accurately represented by a 20% - 80% linear regression of the force-displacement curve, yielding an average R^2 values across all tested rates greater than 0.988 for all the specimens (Figure 3). Across all tested compression rates (V1, V2, and V3) the average R^2 value was 0.996, 0.992, and 0.988 for Lumbar 1, 2, and 3, respectively. Linear stiffness, IVD CSA, and compressive stress values for the whole lumbar spine and segments are given in Table I.

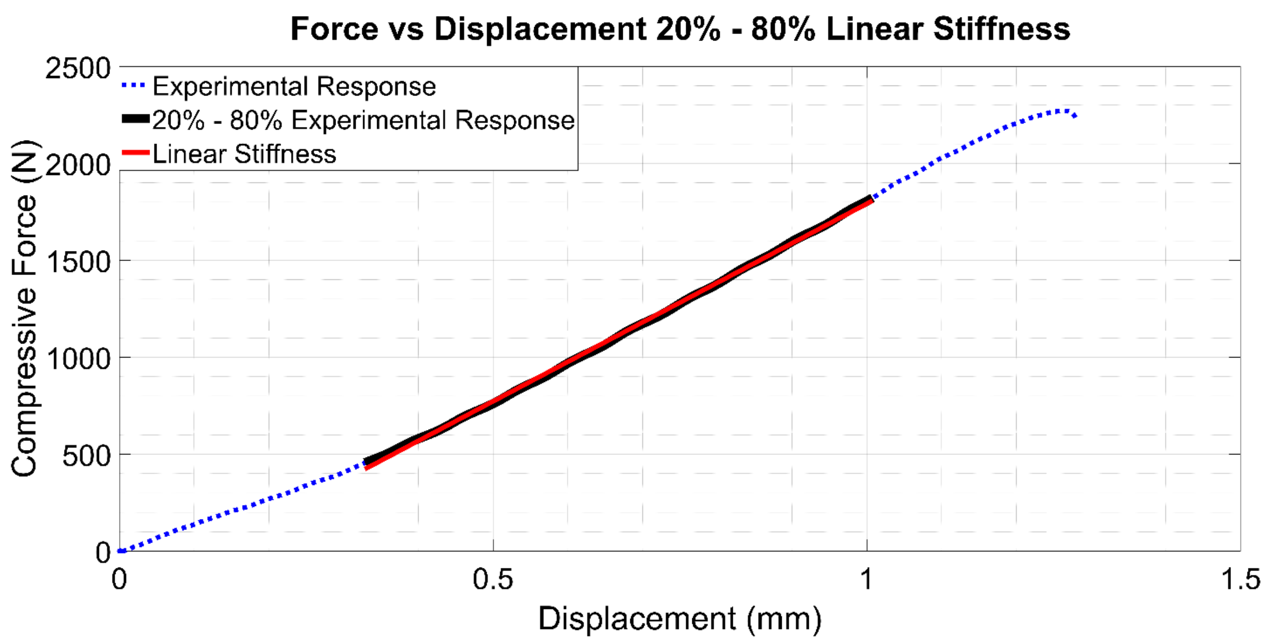

Fig. 3. Linear regression of Force vs. Displacement for a L2-L3 FSU. Region of interest initiated at 20% in order to avoid initial nonlinearity and ended at 80% of the loading profile to avoid including viscoelastic response induced by the deceleration of the hydraulic actuator.

TABLE I
RESULTS FOR LINEAR SPECIMEN'S STIFFNESS, IVD CSA, IVD HEIGHT, AND STRESS VALUES ACROSS TESTED COMPRESSION RATES

Specimen	Segment	Loading Rate	Stiffness (N/mm)	IVD CSA (mm^2)	IVD Height (mm)	σ_{80} (kPa)
Lumbar 1	Thoracolumbar	V1	372.6	2030.6	-	519
		V2	414.1			455.6
		V3	517.9			852.1
	T12-L1	V1	2108	1743.3	10.3	585.9
		V2	2637.4			600.7
		V3	2727.2			546.7
	L2-L3	V1	1656.5	2083.3	12.8	565
		V2	1767.6			536.6
		V3	2005.1			558.6
	L4-S1*	V1	1091.2	2302.8	13.9	640
		V2	1230.8			673.7
		V3	1376.1			671.4
Lumbar 2	Thoracolumbar	V1	445.5	1930.9	-	414.3
		V2	526.6			840.1
		V3	604.2			855.5
	T12-L1	V1	2469.5	1562.3	8.6	462.4
		V2	2630.3			462
		V3	2706.3			550.4
	L2-L3	V1	1515.8	2003.7	11.7	494.4
		V2	1798.6			620.3
		V3	1972.3			632.1
	L4-L5	V1	1788.4	2203.2	14.5	745.1
		V2	1852.4			826.7
		V3	1930.6			830.6
Lumbar 3	Thoracolumbar	V1	261.5	1822.5	-	424.3
		V2	330.2			796.9
		V3	392.5			1204.2
	T12-L1	V1	1529.9	1500.2	7.6	448.8
		V2	1688.1			356.6
		V3	1897.3			345.5
	L2-L3	V1	931.4	2034.6	7.3	578.8
		V2	1255.6			503.4
		V3	1503			428.5
	L4-L5	V1	748	2011.9	7.9	901.6
		V2	1090.3			800.2
		V3	1009.8			589.2

*The L5-S1 IVD was severely calcified, hence the L4-S1 segment was not divided into the L4-L5 FSU. Given CSA and height measurements correspond to L4-L5 IVD.

A one way Anova was made to assess the effects of loading rate on the thoracolumbar spine and tested FSUs stiffness (Figure 4). The loading rate did not demonstrate to have a statistical significant influence on the stiffness behavior for all the FSUs and thoracolumbar spines tested.

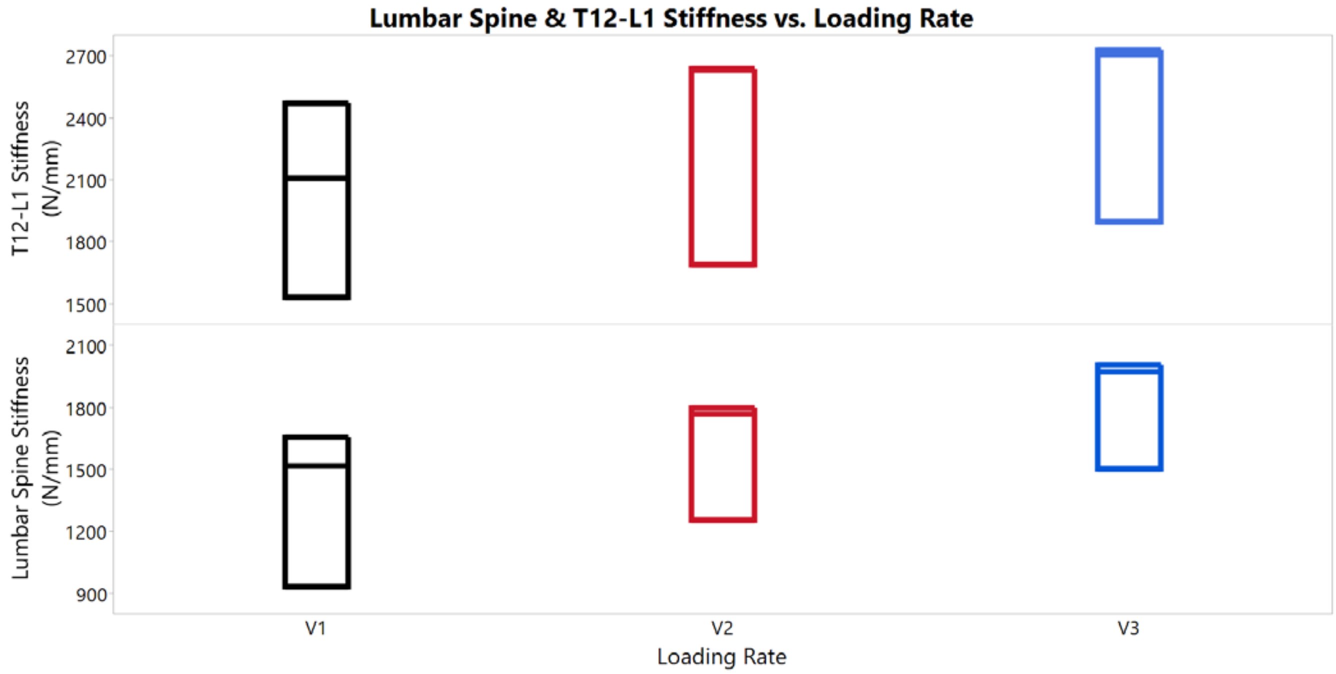

Fig. 4. One way Anova to assess influence of loading rate on thoracolumbar spine and FSU stiffness response. No statistically significant ($p < 0.05$) differences were observed across the tested specimens.

Thoracolumbar Spine Reconstruction

Thoracolumbar spine reconstruction was performed for all tested specimens at the highest compression rate tested (V3). To avoid extrapolation of the experimental data, within a spine specimen, models were developed up to the greatest common compression force experienced across the whole spine and individual FSU tests. The initial nonlinearity response was also discarded for modelling purposes. A fourth order polynomial fit was able to accurately capture the experimental response of all the whole lumbar spines and FSUs, an example fit for Lumbar 2 is given in Fig. 5. The lowest R^2 value amongst all tested specimens was 0.9987 corresponding to the L2-L3 FSU of Lumbar 3.

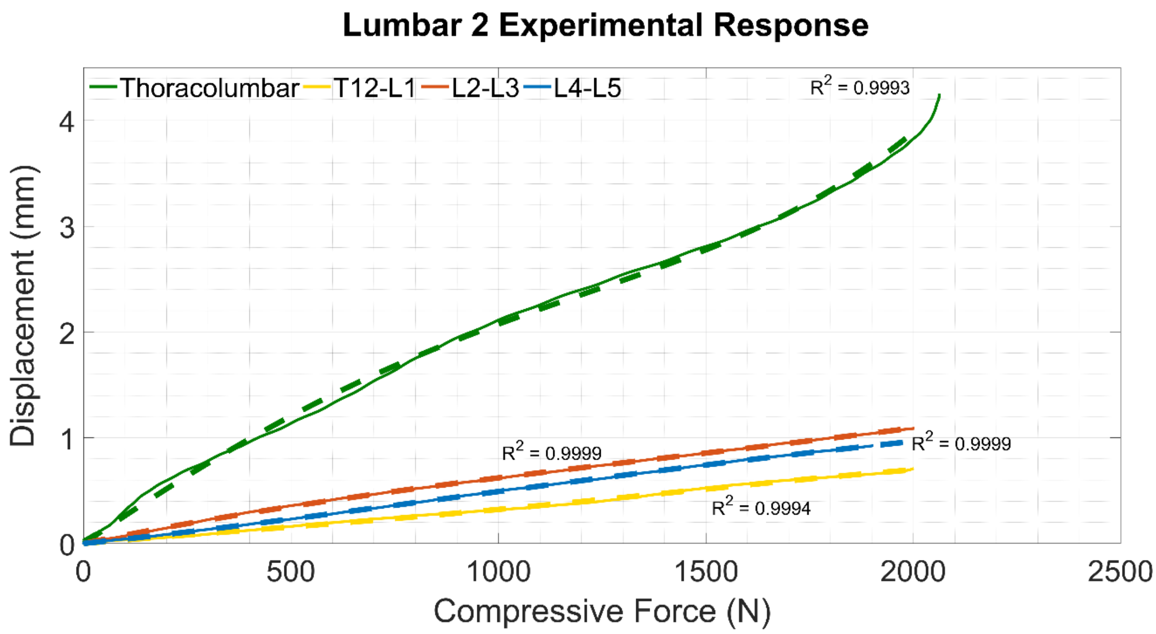

Fig. 5. Fourth order polynomial fits (dashed lines) for Lumbar 2 experimental data (solid lines).

Each thoracolumbar specimen was reconstructed with a combination of FSU experimental data and normalised missing FSU models. Modelled experimental responses and reconstructed spine responses were averaged across the three tested specimens and the standard deviation of the data was used to assess the validity of the composite model within the experimental spine response (Figure 6). A normalised deviation from the mean (Figure 7) was also calculated to assess the accuracy of the reconstructed spine model representation.

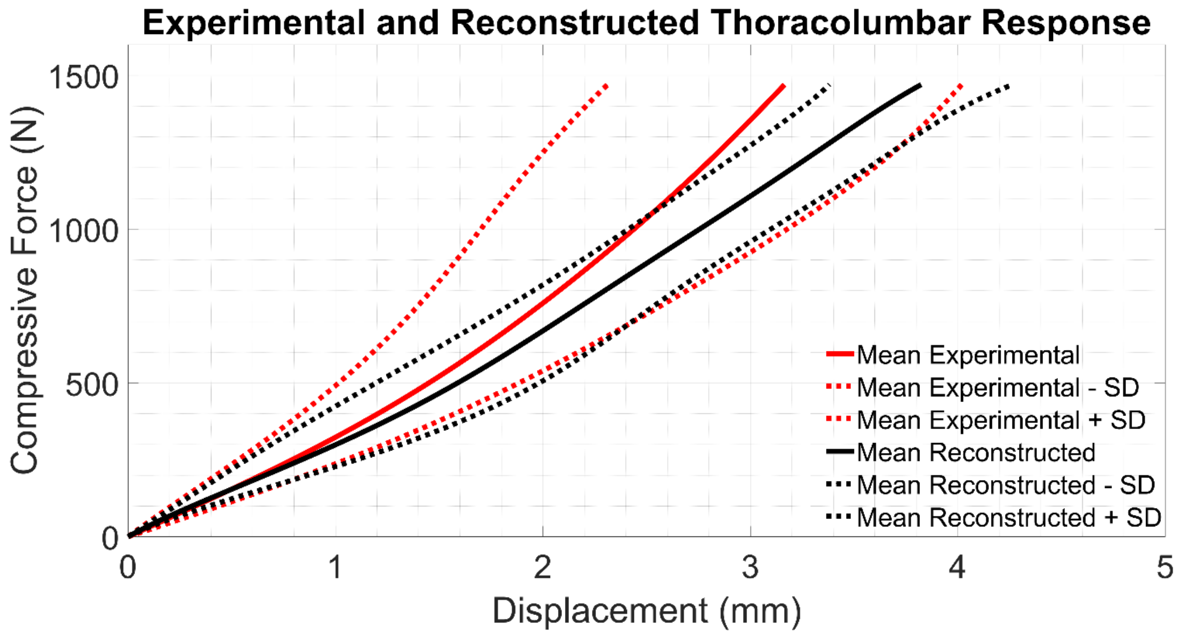

Fig. 6. Modelled experimental and reconstructed thoracolumbar spine response. The deviation from the mean of the reconstruction and the thoracolumbar spine response overlap, but the reconstruction is systematically lower than the thoracolumbar spine response.

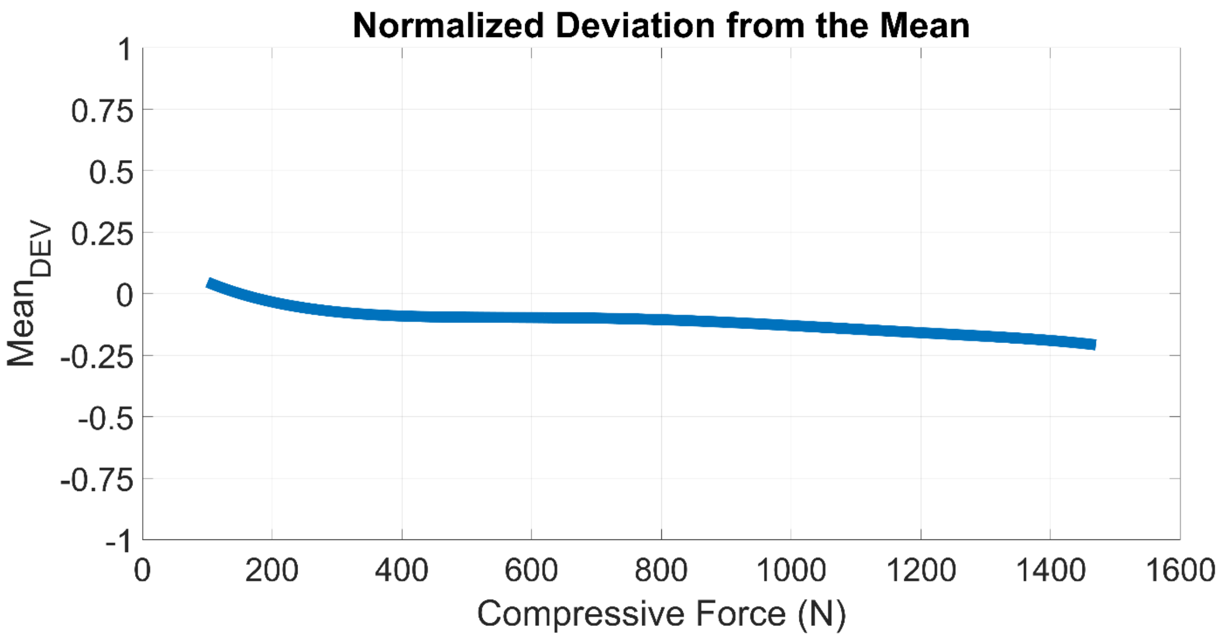

Fig. 7. Normalised deviation from the mean for the mean modelled experimental response and mean reconstructed response. Mean deviation is 8.4%, reaching a maximum over-prediction of 4.7% and maximum under-prediction of 20.8%.

IV. Discussion

The viscoelastic nature of the lumbar spine at low velocity and quasi-static loading conditions has been extensively studied in the literature [14-17]. Other studies have investigated the effects of dynamic loading on the extension-flexion response, load sharing of spinal elements, failure mechanisms, and injury probability of the lumbar spine [6,27-29]. Reference [8] assessed the biomechanical response of the lumbar spine under dynamic compression at velocities of 0.1 m/s, but the influence of a range of compression rates on the lumbar spine response was not pursued. In this study, the same thoracolumbar spine specimen was subjected to a range of dynamic compression rates to elucidate its influence over the lumbar spine stiffness response. A linear regression of 20% - 80% of the force-displacement response was found to be a good representation of the stiffness behaviour of both whole lumbar spines and segments (Figure 3), with R^2 values averaging 0.992 ± 0.004 for all specimens tested at all compression rates.

As expected, segment stiffness was greater than thoracolumbar stiffness, with FSU stiffness ranging from 2444 ± 473 N/mm for T12-L1 at V3, to 1268 ± 736 N/mm for L4-L5 at V1. Similarly to the segmental stiffness response the thoracolumbar spines exhibited stiffness of 360 ± 93, 424 ± 99, 505 ± 106 N/mm for V1, V2, and V3, respectively. While segmental stiffness was found to decrease in the cranio-caudal direction with T12-L1 being the stiffest FSU, compressive stress increased in the cranio-caudal direction. These results agree with findings reported by [15]. Following Hooke's Law principle [30], within the same stress conditions the stiffness of a material is inversely proportional to the strain it is subjected to. Given that FSU height increases in the cranio-caudal direction we expect the stiffness of the FSU to decrease. Furthermore, when the FSUs are combined in a linear model as a series of springs in series to recreate thoracolumbar spine behaviour we verify that the whole spine response is less stiff than that of the FSUs separately. However, the cranio-caudal increase of the IVD CSA outweighs the decrease of segmental stiffness, thus yielding an increased compressive strength in the cranio-caudal direction.

A one way Anova (Figure 4) showed that the investigated loading rates do not have a statistically significant influence on the stiffness response for both thoracolumbar spines and FSUs. However, it suggests a correlation of increased stiffness with increasing loading rate, which is expected for a viscoelastic material, this was true for both thoracolumbar spines and FSUs tested. The loading-rate dependent behavior of the lumbar spine and FSUs during dynamic compression is dominated by the IVD due to the anisotropic properties of the annulus fibrosus and nucelous pulposus water content, which characterise the viscoelastic nature of the IVD [31]. It is worth noting that this study was performed on a limited sample size of thoracolumbar spine specimens and within a limited range of loading rates. In addition, the influence of age or IVD water content on the viscoelastic response of the thoracolumbar and FSUs were not characterized as part of this study. Therefore, the trends discussed should be taken only as initial suggestion of a correlation of the thoracolumbar spine and FSUs dynamic compressive behaviour and loading rate. More specimens need to be studied to verify and quantify this behavior more accurately and to determine if a statistical significant difference can be observed beyond the intra-specimen variability across the proposed loading rates. Furthermore, it is expected that expanding the range of investigated loading rates by orders of magnitude will accentuate the loading rate dependence of the thoracolumbar spine and FSUs compressive response as it has been shown in the intervertebral discs [12].

Estimating the thoracolumbar spine response from FSU data has inherit limitations due to the nature of FSU testing. Reference [19] proposed a linear and logarithmic approach with frame-compliance correction to reconstruct whole cervical spine data from FSU tests under tensile loading. They assumed the missing FSU stiffness for the upper cervical spine (UCP) to be equal to tested FSU of the UCP, and missing FSU stiffness for the lower cervical spine (LCS) to be equal to tested LCS segments. Correction of stiffness from frame compliance reduced the error between whole and reconstructed spine models; however, the full spine response could not be achieved from FSU data. Similarly, when analysing whole cervical spine and FSU tensile data from [20], the stiffness response from the linear reconstructed spine only achieves 58% of the tested whole spine, when assuming that the missing FSUs are equal to the stiffest tested segment. In this study, if the thoracolumbar spine response was reconstructed from FSUs using a linear combination of the compliance of six segments (Table 1), where missing segment compliance is approximated as the mean compliance of the superior and inferior tested segments. Results of the linear model will not recreate the thoracolumbar response, with reconstructed stiffness averaging 63% of thoracolumbar spine linear stiffness. This may be attributed to differences in nonlinear viscoelastic response in the lumbar segments compared with the thoracolumbar spine. Owing to response and area differences between segments, the stress-strain conditions in the segments are not fully replicated in the thoracolumbar spine stress-strain response, leading to an under-prediction of the reconstructed response. Therefore, a nonlinear approach was pursued to reconstruct whole spine response, by modelling the FSU and thoracolumbar spine experimental data with a fourth order polynomial, corrected for nonlinear fixation compliance, to capture the nonlinearities of individual testing (Figure 5). Unknown FSU response was approximated with a normalised criteria that incorporated both superior and inferior known segment response and their anatomical properties (CSA and height) to provide a more precise weighted response that also incorporates force distribution (through CSA) and displacement (through IVD height) contributions of the unknown segment. Figure 6 shows how the mean proposed nonlinear reconstruction overlaps within the intra-specimen variability of the modelled experimental spine, without completely replicating it. The normalised deviation from the mean (Figure 7) ranges between 4.7% and -20.8% with a mean reconstructed response of 91.6% of the experimental response. The reconstructed model underpredicts the experimental thoracolumbar response for the most part and its deviation from the mean increases with axial force. The $\mathrm{Mean}_{\mathrm{DEV}}$ suggests that on average the nonlinear reconstruction outperforms the linear model reconstruction by 28.6%. The surpassing of the nonlinear, fixation compensated and normalised missing segment composite model over a linear combination model highlights the importance of characterising the relationship between lumbar FSUs and the thoracolumbar spine, and capturing the nonlinearities of the FSU experimental response. Remaining differences could be attributed to changes in boundary conditions from whole spine to segment testing, which could influence the recruitment of facets and ligaments and introduce changes in the segmental behaviour in comparison with the thoracolumbar spine response.

V. CONCLUSIONS

This study assesses the influence of dynamic compression rates for a range of underbody blast conditions of the thoracolumbar spine, providing initial evidence that investigated rates do not cause a statistical significant difference on the stiffness of the thoracolumbar spine. Nevertheless, a correlation of increased stiffness with increasing loading rate for both thoracolumbar and FSU specimens is suggested. Furthermore, it is the first study that corroborates that, like the cervical spine in tension, composite models of the lumbar spine from FSU data underpredict the thoracolumbar spine response during dynamic compression. However, we proposed a nonlinear model that takes into account the differences of force-displacement behaviour of FSUs when tested individually and introduced an anatomical-based normalisation to approximate untested FSU responses. The nonlinear reconstruction of whole spine data outperforms a linear reconstruction approach, getting us closer to achieve full thoracolumbar spine behaviour reconstruction from FSU response under dynamic compression. Even though the nonlinear composite response underpredicts the thoracolumbar spine response at some stages of the loading profile, it is important to note that the deviation from the mean of the nonlinear model overlaps with the standard deviation of the experimental response of the three thoracolumbar spines tested. Increasing the sample size of this study could further ratify and improve the proposed nonlinear model's predicting capabilities.

VI. ACKNOWLEDGEMENT

The authors would like to acknowledge Jason R. Kait from the Injury Biomechanics Laboratory at Duke University for his collaboration in experiment preparation and data acquisition. Furthermore, the authors thank the Graduate School, Department of Biomedical Engineering, and the Pratt Fellows Program of Duke University, USA, for their contributions to this work.

VII. REFERENCES

[1] Harrop, J.S., Sharan, A.D., Vaccaro, A.R., and Przybylski, G.J. The Cause of Neurologic Deterioration After Acute Cervical Spinal Cord Injury. *Spine*, 2001. 26(4): p. 340-346

[2] Sekhon, L.H.S. and Fehlings, M.G. Epidemiology, Demographics, and Pathophysiology of Acute Spinal Cord Injury. *Spine*, 2001. 26(24S): p. S2-S12

[3] Kang, D.G., Lehman, R.A., Jr., and Carragee, E.J. Wartime spine injuries: understanding the improvised explosive device and biophysics of blast trauma. *The Spine Journal*, 2012. 12(9): p. 849-857

[4] Loftis, K.L., Mazuchowski, E.L., Clouser, M.C., and Gillich, P.J. Prominent injury types in vehicle underbody blast. *Military medicine*, 2019. 184(Supplement_1): p. 261-264

[5] Blair, J.A., Patzkowski, J.C., et al. Spinal column injuries among Americans in the global war on terrorism. *J Bone Joint Surg Am*, 2012. 94(18): p. e135(1-9)

[6] Duma, S.M., Kemper, A.R., McNeely, D.M., Brolinson, P.G., and Matsuoka, F. Biomechanical response of the lumbar spine in dynamic compression. *Biomedical sciences instrumentation*, 2006. 42: p. 476-481
[7] Stemper, B.D., Storvik, S.G., et al. A New PMHS Model for Lumbar Spine Injuries During Vertical Acceleration. *Journal of Biomechanical Engineering*, 2011. 133(8): p. 081002-081002-9
[8] Demetropoulos, C.K., Yang, K.H., Grimm, M.J., Khalil, T.B., and King, A.I. Mechanical properties of the cadaveric and Hybrid III lumbar spines. *SAE transactions*, 1998: p. 2862-2871
[9] Yoganandan, N., Moore, J., et al. Human lumbar spinal column injury criteria from vertical loading at the base: Applications to military environments. *Journal of the Mechanical Behavior of Biomedical Materials*, 2020: p. 103690
[10] Arun, M.W., Hadagali, P., et al. Biomechanics of lumbar motion-segments in dynamic compression. 2017, SAE Technical Paper.
[11] Newell, N., Carpanen, D., Grigoriadis, G., Little, J.P., and Masouros, S.D. Material properties of human lumbar intervertebral discs across strain rates. *The Spine Journal*, 2019. 19(12): p. 2013-2024
[12] Kemper, A.R., McNally, C., and Duma, S.M. The influence of strain rate on the compressive stiffness properties of human lumbar intervertebral discs. *Biomedical sciences instrumentation*, 2007. 43: p. 176-181
[13] Chowdhury, M.R. and Crawford, D.M., "Dynamic Behavior of Materials, Volume 1", pages 57-61, Springer, 2018
[14] Pintar, F.A., Yoganandan, N., Myers, T., Elhagediab, A., and Sances Jr, A. Biomechanical properties of human lumbar spine ligaments. *J. Biomech.*, 1992. 25(11): p. 1351-1356
[15] Brinckmann, P., Biggemann, M., and Hilweg, D. Prediction of the compressive strength of human lumbar vertebrae. *Clinical Biomechanics*, 1989. 4: p. iii1-iv27
[16] Adams, M. and Dolan, P. A technique for quantifying the bending moment acting on the lumbar spine in vivo. *J. Biomech.*, 1991. 24(2): p. 117-126
[17] Schmidt, A.L., Paskoff, G., Shender, B.S., and Bass, C.R. Risk of lumbar spine injury from cyclic compressive loading. *Spine*, 2012. 37(26): p. E1614-E1621
[18] Lucas, S.R., Bass, C.R., et al. Viscoelastic properties of the cervical spinal ligaments under fast strain-rate deformations. *Acta Biomaterialia*, 2008. 4(1): p. 117-125
[19] Nightingale, R.W., Chancey, V.C., et al. The Human Cervical Spine in Tension: Effects of Frame and Fixation Compliance on Structural Responses. *Traffic Injury Prevention*, 2004. 5(2): p. 151-155
[20] Luck, J.F., Nightingale, R.W., et al. Tensile Mechanical Properties of the Perinatal and Pediatric PMHS Osteoligamentous Cervical Spine. *Stapp Car Crash Journal*, 2008. 52: p. 107-134
[21] Luck, J.F., Nightingale, R.W., et al. Tensile Failure Properties of the Perinatal, Neonatal, and Pediatric Cadaveric Cervical Spine. *Spine*, 2013. 38(1): p. E1-E12
[22] Galante, J.O. Tensile properties of the human lumbar annulus fibrosus. *Acta Orthopaedica Scandinavica*, 1967. 38(sup100): p. 1-91
[23] Sedlin, E.D. and Hirsch, C. Factors affecting the determination of the physical properties of femoral cortical bone. *Acta Orthopaedica Scandinavica*, 1966. 37(1): p. 29-48
[24] Tkaczuk, H. Tensile properties of human lumbar longitudinal ligaments. *Acta Orthopaedica Scandinavica*, 1968. 39(sup115): p. 1-69
[25] Reed, M.P. and Ebert, S.M. The seated soldier study: posture and body shape in vehicle seats. 2013
[26] Smeathers, J. and Joanes, D. Dynamic compressive properties of human lumbar intervertebral joints: a comparison between fresh and thawed specimens. *J. Biomech.*, 1988. 21(5): p. 425-433
[27] Demetropoulos, C.K., Yang, K.H., Grimm, M.J., Artham, K.K., and King, A.I. High rate mechanical properties of the Hybrid III and cadaveric lumbar spines in flexion and extension. 1999, SAE Technical Paper.
[28] Wagnac, E., Arnoux, P.-J., Garo, A., and Aubin, C.-E. Finite element analysis of the influence of loading rate on a model of the full lumbar spine under dynamic loading conditions. *Medical & biological engineering & computing*, 2012. 50(9): p. 903-915
[29] Yoganandan, N., DeVogel, N., et al. Human lumbar spine responses from vertical loading: ranking of forces via Brier score metrics and injury risk curves. *Annals of biomedical engineering*, 2020. 48(1): p. 79-91
[30] Lakes, R.S., "Viscoelastic Solids (1998)". 2017: CRC press.
[31] McNally, D. and Adams, M.A. Internal intervertebral disc mechanics as revealed by stress profilometry. *Spine*, 1992. 17(1): p. 66-73

VIII. APPENDIX

TABLE A.I

FOURTH ORDER POLYNOMIAL COEFFICIENTS FOR EXPERIMENTAL THORACOLUMBAR SPINES AND SPINAL SEGMENTS.

Specimen	Segment	$a * 10^{-13}$	$b * 10^{-9}$	$c * 10^{-6}$	$e * 10^{-3}$
Lumbar 1	Thoracolumbar	-5.4	2.5	-4	4.5
	T12-L1	-51	21	-28	52
	L2-L3	-65	32	-58	94
	L4-S1	590	520	-39	1.3
Lumbar 2	Thoracolumbar	2.7	-59	-26	2.7
	T12-L1	-35	13	-11	34
	L2-L3	-230	640	-25	81
	L4-L5	12	-860	16	40
Lumbar 3	Thoracolumbar	-5.6	1.9	-3.1	5.3
	T12-L1	1.7	-56	55	45
	L2-L3	15	18	-79	1.5
	L4-L5	-5.6	2.4	-3.4	2.6